Optimal Sequencing and Motion Control in a Roundabout with Safety Guarantees

Yingqing Chen, Christos G. Cassandras and Kaiyuan Xu

Abstract— We develop controllers for Connected and Automated Vehicles (CAVs) traversing a single-lane roundabout so as to simultaneously determine the optimal sequence and associated optimal motion control jointly minimizing travel time and energy consumption while providing speed-dependent safety guarantees, as well as satisfying velocity and acceleration constraints. This is achieved by integrating (a) Model Predictive Control (MPC) to enable receding horizon optimization with (b) Control Lyapunov-Barrier Functions (CLBFs) to guarantee convergence to a safe set in finite time, thus providing an extended stability region compared to the use of classic Control Barrier Functions (CBFs). The proposed MPC-CLBF framework addresses both infeasibility and myopic control issues commonly encountered when controlling CAVs over multiple interconnected control zones in a traffic network, which has been a limitation of prior work on CAVs going through roundabouts, while still providing safety guarantees. Simulations under varying traffic demands demonstrate the controller's effectiveness and stability.

I. INTRODUCTION

It has been well documented that urban congestion has reached critical levels in terms of time, pollution, and fuel consumption [1]. The emergence of Connected and Automated Vehicles (CAVs) along with real-time communication between mobile endpoints and the infrastructure [2] make it possible to achieve smoother traffic flow through better information utilization and trajectory design.

Most research to date has focused on the control and coordination of CAVs within a single *Control Zone* (CZ) that encompasses a conflict area such as merging roadways, [3], lane changing [4] and unsignalized intersections [5]. However, the transition from a single CZ to multiple interconnected CZs is particularly challenging [6]: while in an isolated CZ it is assumed that vehicle states initially satisfy all constraints upon entering this CZ, when several CZs are interconnected it is generally the case that the state of a vehicle exiting one CZ does not satisfy the next CZ's constraints. Additionally, since the traffic flow is propagated throughout a network of CZs, myopic optimal control limited to one CZ may require extra control effort in the next and even cause congestion if CZs are in close proximity, resulting in blocked traffic. Thus, directly applying control techniques used in a single CZ to multiple CZs without considering system-wide or local neighboring traffic information leads

to performance degradation and lack of safety guarantees, especially when the CZs are tightly coupled.

A typical case in point of interconnected CZs arises in a roundabout, a configuration which is attractive to traffic control because its geometry enhances safety by promoting lower speeds, better visibility, increased reaction time for drivers, and resulting in less severe crashes when they occur [7]. Though roundabouts offer many such benefits, their effective implementation requires more careful planning, since the compact geometry with multiple closely-spaced Merging Points (MPs) requires tighter control and more stringent safety constraint satisfaction. Both model-based [8]–[10] and learning-based methods [11], [12] have been considered to deal with the control and coordination of CAVs at roundabouts (see [13] for details). In order to improve computational efficiency, a joint Optimal Control and Control Barrier Function (OCBF) approach is used in [14] such that unconstrained control trajectories are optimally tracked while also guaranteeing the satisfaction of all constraints using Control Barrier Functions (CBFs). In addition, in order to optimize the estimated future performance, Model Predictive Control (MPC) is used in [15] and [8].

However, these works fall short of addressing the control issues that arise in interconnected CZs as described earlier. Learning-based methods are reward-driven and cannot reliably prevent conflicts between vehicles. Among model-based techniques, some fail to account for the tightly coupled conflict structure and regard a roundabout as consisting of multiple independent CZs, prone to safety violation, energy waste, and congestion. Our previous work [6] deals with the infeasibility as vehicles progress through successive CZs by defining a Feasibility Enforcement (FE) mode within which a maximum deceleration is set. This approach sacrifices considerable energy to enforce feasibility, inefficient that can be avoided with proper control. Therefore, the first contribution of this paper is to propose a decentralized MPC-CLBF framework which leverages the coupled structure of multiple interconnected CZs and addresses both infeasibility and myopic control issues. When constraints from the next CZ are not satisfied for vehicles entering that CZ, we use *Control Lyapunov-Barrier Functions* (CLBFs) [16] to ensure convergence back to a safe set in *finite* time, thus providing an extended stability region relative to classic CBFs. In order to overcome the myopic nature of prior CBF-based controllers, Model Predictive Control (MPC) is used to account for future performance across different CZs, therefore achieving optimality over a tunable receding horizon.

The second contribution of this paper is to consider

Y. Chen, C. G. Cassandras and K. Xu are with the Division of Systems Engineering and Center for Information and Systems Engineering, Boston University, Brookline, MA 02446 {yqchenn;cgc;xky}@bu.edu.
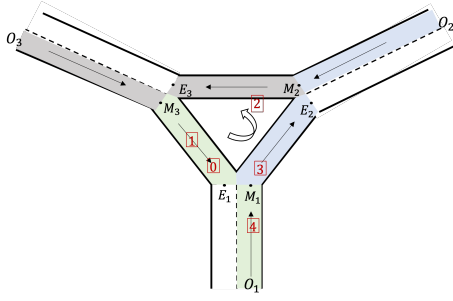
Fig. 1: A roundabout with 3 entries

the *joint* solution of the sequencing and motion control problems. The problem of sequencing vehicles through a roundabout has been dealt with by mostly assuming that CAVs maintain a FIFO order, which has been shown to be often inefficient [17]. This assumption is replaced by other sequencing schemes [14], but they fail to consider control after merging, thus not able to ensure optimal coordination over interconnected CZs. Our proposed solution combines an optimal sequencing process with the MPC-CLBF framework mentioned above so as to select an optimal sequence and motion control of each CAV in this sequence to jointly optimize the future vehicle speed and its energy consumption while guaranteeing safety.

II. PROBLEM FORMULATION

We consider a single-lane triangle-shaped roundabout with N entry and N exit points where $N \geq 2$. For simplicity we limit our analysis here to $N = 3$, as depicted in Fig. 1, with straightforward extensions to $N > 3$. We chose a triangular geometry to simplify the analysis, focusing on the joint sequencing and motion control problem; the extension to circular roundabouts complicates things, but can still be handled as demonstrated in [18]. Additionally, implementing a triangular layout enables us to carry out direct performance comparisons to prior results using a similar configuration in [14] so as to evaluate the advantages of the joint sequencing and motion control approach developed in this paper with all traffic consisting of CAVs. Thus, as in [14], we consider the case where all traffic consists of CAVs which randomly enter the roundabout from three different origins O_1, O_2 and O_3 and have randomly assigned exit points E_1, E_2 and E_3. We assume all CAVs move in a counterclockwise way.

The entry road segments are connected with the triangle at the three Merging Points (MPs) labeled as M_1, M_2 and M_3, where CAVs from different road segments may potentially collide with each other. Centered at each MP, we partition the roundabout into three Control Zones (CZs), labeled CZ_1, CZ_2 and CZ_3, and shaded in green, blue, grey respectively in Fig.1. Each CZ includes two road segments towards the corresponding MP: one is the entry road indexed by 1, and the other is the segment within the roundabout, indexed by 0. Thus, we define $c_i \in \{0, 1\}$ as the road segment where CAV i is currently located, where $c_i = 1$ indicates CAV i is at an entry road, otherwise $c_i = 0$. We also assume that all road

segments have the same length L (extensions to different lengths are straightforward). The full trajectory of a CAV in terms of the MPs it must go through can be determined by its entry and exit points.

The vehicle dynamics for each CAV $i \in S(t)$ along the road segment to which it belongs take the form

$$\begin{bmatrix} \dot{x}_i(t) \\ \dot{v}_i(t) \end{bmatrix} = \begin{bmatrix} v_i(t) \\ u_i(t) \end{bmatrix} \tag{1}$$

where $x_i(t)$ denotes the distance from the origin of the road segment where CAV i currently locates, $v_i(t)$, $u_i(t)$ denotes the velocity and acceleration respectively. We limit our discussion to simple dynamics to emphasize the proposed framework. More advanced dynamics can be used to refine the control without affecting the core effectiveness (see [19]).

Let $S(t)$ be the set of indices of CAVs present in the roundabout at time t. The cardinality of $S(t)$ is denoted by $N(t)$. When a new CAV arrives at the roundabout, it is assigned the index $N(t) + 1$. Each time a CAV i leaves the roundabout, it is removed from $S(t)$ and all CAV indices larger than i decrease by 1. We then partition $S(t)$ into subsets based on their current CZ and define a merging group as a set of CAVs present at the same CZ at time t. Let $S_k(t)$, $k \in \{1, 2, 3\}$, be the set of indices of CAVs (from $S(t)$) within the merging group of CZ_k at time t, where $S_1(t) \cap S_2(t) \cap S_3(t) = \emptyset$, $S(t) = S_1(t) \cup S_2(t) \cup S_3(t)$. The cardinality of $S_k(t)$ is denoted by $N_k(t)$ with $k \in \{1, 2, 3\}$.

The Coordinator Table. A coordinator table is used for each CZ to record the essential state information for all CAVs within it, and to identify all conflicting CAVs under a given merging sequence. An example of such table corresponding to Fig. 1 for CZ_1 is shown in Table I. The definition of each column is as follows: *idx* is the unique CAV index at the roundabout; *state* is the CAV state $\mathbf{x_i} = (x_i, v_i)$ where x_i is the distance to the location of CAV i from the entry point of its current road segment and v_i is the velocity of CAV i; *initial CZ* is the index of the CZ from which CAV i enters the roundabout; *final CZ* is the index of the CZ through which CAV i exits the roundabout; *current CZ* is the index of the CZ where CAV i is currently located; c_i is the classification index of the road segment where CAV i is currently located: $c_i = 1$ for an entry segment and $c_i = 0$ for the segment within the roundabout; i_p is the index of the CAV which physically immediately precedes CAV i in the roundabout (if one exists), noting that CAV i_p is not necessarily located in the same CZ as CAV i; i_m is the index of the last CAV that precedes CAV i (if one exists) at the next MP within a given sequence. CAV i_m must be in the same CZ but a different road segment than that of CAV i, i.e., $c_i \neq c_{i_m}$.

The three coordinator tables $S_k(t)$, $k \in \{1, 2, 3\}$, are up-

TABLE I: The Coordinator Table $S_1(t)$

$S_1(t)$							
idx	state	initial CZ	final CZ	current CZ	c_i	i_p	i_m
0	$\mathbf{x_0}$	3	1	1	0		
1	$\mathbf{x_1}$	3	2	1	0	0	4
4	$\mathbf{x_4}$	1	2	1	1	3	

dated simultaneously in an event-driven manner. The detailed triggering events and logic can be found in [13].

A. Optimal Control Problem (OCP)

We consider two objectives for each CAV subject to four constraints, as detailed next.

Objective 1 Minimize the travel time $J_{i,1} = t_i^f - t_i^0$ where t_i^0 and t_i^f are the times CAV i enters and exits the roundabout.

Objective 2 Minimizing energy consumption:

$$J_{i,2} = \int_{t_i^0}^{t_i^f} C(u_i(t))dt, \tag{2}$$

where $C(\cdot)$ is a strictly increasing function since the energy consumption rate is a monotonic function of the acceleration.

Constraint 1 (Rear end safety constraints): Let i_p denote the index of the CAV which physically immediately precedes i in the roundabout (if one is present), whether they are at the same CZ or not. We define the distance $z_{i,i_p}(t) := \bar{x}_{i_p}(t) - x_i(t)$ where $\bar{x}_{i_p}(t) = x_{i_p}(t) + L\Delta$ if CAV i_p and CAV i are at different CZs and the CZ difference is Δ (taken counterclockwise); otherwise $\bar{x}_{i_p}(t) = x_{i_p}(t)$. We require:

$$z_{i,i_p}(t) \geq \varphi v_i(t) + \delta, \quad \forall t \in [t_i^0, t_i^f], \tag{3}$$

where $v_i(t)$ is the speed of CAV $i \in S(t)$ and φ denotes the reaction time (as a rule, $\varphi = 1.8$s is used, e.g., [20]). If we define z_{i,i_p} to be the distance from the center of CAV i to the center of CAV i_p, then δ is a constant determined by the length of these two CAVs (generally dependent on i and i_p but taken to be a constant for simplicity).

Constraint 2 (Safe merging constraint): Let i_m denote the index of the CAV traveling on a different road segment of the same CZ that shares the same next MP, M_k, as CAV i. CAV i_m directly precedes CAV i in arriving at M_k among all vehicles in its segment under a given crossing sequence. Let $t_{i_m}^k, k \in \{1,2,3\}$ be the arrival time of CAV i_m at MP M_k. The distance between i_m and i, given by $z_{i,i_m}(t) \equiv x_{i_m}(t) - x_i(t)$, is constrained by

$$z_{i,i_m}(t_{i_m}^k) \geq \varphi v_i(t_{i_m}^k) + \delta, \forall i \in S(t), k \in \{1,2,3\} \tag{4}$$

Constraint 3 (Vehicle limitations): There are constraints on the speed and acceleration for each $i \in S(t)$, i.e.,

$$v_{\min} \leq v_i(t) \leq v_{\max}, \forall t \in [t_i^0, t_i^f], \tag{5}$$

$$u_{i,\min} \leq u_i(t) \leq u_{i,\max}, \forall t \in [t_i^0, t_i^f], \tag{6}$$

where $v_{\max} > 0$, $v_{\min} \geq 0$, $u_{i,\min} < 0$ and $u_{i,\max} > 0$ denote the speed and control limits respectively.

Problem 1: Our goal is to determine a control law to achieve objectives 1-2 subject to constraints 1-3 for each $i \in S(t)$ governed by the dynamics (1). Thus, we combine Objectives 1-2 by constructing a convex combination:

$$J_i(u_i(t)) := \beta(t_i^f - t_i^0) + \int_{t_i^0}^{t_i^f} \frac{1}{2} u_i^2(t)dt, \tag{7}$$

where $\beta \geq 0$ is a weight factor that can be adjusted to penalize travel time relative to the energy cost, subject to (1), (3)-(6) given $t_i^0, x_i(t_i^0), v_i(t_i^0)$.

Obviously, solving this problem for any CAV i requires knowledge of i_p and i_m in (3)-(4) whose assignment is dynamically changing, especially when a CAV changes CZs.

Our goal is to determine an optimal sequence for each merging group of CAVs, which is centrally determined by the coordinator, while also determining the corresponding optimal control $u_i(t)$, which is calculated in a decentralized manner.

III. OPTIMAL SEQUENCING AND MOTION CONTROL

We propose a joint sequencing and motion control process that comprises three parts: (a) determine all feasible sequences that all CAVs in a CZ can follow when crossing its MP, (b) evaluate each candidate feasible sequence using the MPC-CLBF framework, and (c) determine the optimal sequence and associated control for each CAV.

Feasible Sequences. A feasible sequence is a prioritized list of indices for all CAVs currently within the same CZ, ordered by projected CZ exit times (either progressing to the next CZ or leaving the roundabout). Given the single lane assumption (which excludes overtaking), the sequence must maintain relative on-road precedence. The CAVs not located at their final CZ can conflict with CAVs from other inbound road segments heading to the shared next MP. Thus, the relative merging order of CAVs is flexible, comprising the feasible set of sequences to evaluate. We denote the set of all feasible sequences for CZ_k at time t as $F_k(t)$. For example, the feasible sequences for $S_1(t)$ as shown in Table I are $F_1(t) = \{[0,1,4], [0,4,1], [4,0,1]\}$. Each feasible sequence is equivalent to a pair of i_p, i_m assignments for each i. See [13] for the detailed assignment process.

Evaluate a Feasible Sequence. For each merging group in $CZ_k, k \in \{1,2,3\}$, we need to evaluate each feasible sequence $\mathbf{f} \in F_k(t)$ determined above, which is associated with a specific pair of i_p and i_m assignments for every i in this sequence. Thus, we need to evaluate the performance of each CAV $i \in \mathbf{f}$ under optimal motion control.

1) Optimal Control of Single CAV: We start with the *unconstrained* optimal control solution of (7) when safety constraints (3) and (4) are inactive. This has been derived in prior work [14] based on a standard Hamiltonian analysis.

However, if i_p or i_m exists, the constrained optimal control problem becomes hard to solve as multiple constraints can become active. To overcome this, Control Barrier Functions (CBFs) have been used [21] for three main reasons: (a) The original constraints (3)-(6) can be replaced by CBF-based constraints that imply (3)-(6), hence they guarantee their satisfaction, (b) the forward invariance property of CBFs guarantees constraint satisfaction over all future times, (c) the new CBF-based constraints are *linear* in the control, which drastically reduces the computational cost of determining them and enables real-time implementation. In particular, based on the vehicle dynamics (1), we define $f(\boldsymbol{x}_i(t)) = [v_i(t), 0]^T, g(\boldsymbol{x}_i(t)) = [0,1]^T$. Each of the constraints (3)-(6) can be expressed in the form $b_j(\boldsymbol{x}_i(t)) \geq 0, j \in 1, 2, \ldots$ and the CBF method maps $b_j(\boldsymbol{x}_i(t)) \geq 0$ into a new constraint which directly involves the control $u_i(t)$ and takes the form

$$L_f b_j(\boldsymbol{x}_i(t)) + L_g b_j(\boldsymbol{x}_i(t))u_i(t) + \gamma_j(b_j(\boldsymbol{x}_i(t))) \geq 0 \tag{8}$$

where L_f, L_g denote the Lie derivatives of $b_j(\boldsymbol{x}_i(t))$ along f and g respectively and $\gamma_j(\cdot)$ denotes some class-$\mathcal{K}$ function (in practice, a linear class-$\mathcal{K}$ function is often used). This CBF-based constraint is a sufficient condition for $b_j(\boldsymbol{x}_i(t)) \geq 0$ (see [21]) and may, therefore, be conservative depending on the choice of $\gamma_j(\cdot)$.

With CBF-based constraints of the form (8) replacing the original ones, the new OCP can be efficiently solved by discretizing time and solving a simple Quadratic Program (QP) over each time step (details can be found in [21]) exploiting the linearity in u in (8). One limitation of this approach is that it is "myopic" in the sense that the control determined at a specific time step cannot ensure that all constraints remain satisfied at future steps (e.g., they may conflict with the control constraints in (6)). Given the roundabout's compact geometry which couples closely-spaced MPs, control actions propagate rapidly across different CZs and this myopic nature of control selection becomes inadequate. This motivates the two new elements we bring to the solution of this problem. First, we use a receding-horizon MPC framework to evaluate future performance not only over a single time step, but over a receding horizon H of multiple lookahead steps. The choice of H improves accuracy at the expense of computational cost. Second, we address the problem of a CAV entering the next CZ in its path without necessarily satisfying the safety constraints required in this new CZ. We resolve this issue through the use of *Control Lyapunov-Barrier Functions (CLBFs)* instead of basic CBFs, which allows us to ensure the satisfaction of these constraints within a properly selected finite time interval.

2) MPC-based optimal control problem solution: Starting from current time t, we discretize time using time steps of equal length T_d. The dynamics are also discretized and we set $\boldsymbol{x}_{i,h} = \boldsymbol{x}_i(t + h \cdot T_d)$ where $h = 1, 2, \dots$ is the hth time step since t. The decision variables $u_{i,h} = u_i(t+(h-1)\cdot T_d)$ are assumed to be constant over each time step. Therefore, we set the control, velocity, position trajectory over next H time steps as a vector respectively: $\mathbf{u}_i = [u_{i,1}, \dots u_{i,H}]$, $\mathbf{v}_i = [v_{i,1}, \dots v_{i,H}]$ and $\mathbf{x}_i = [x_{i,1}, \dots x_{i,H}]$. When adopting sequence $\mathbf{f}$, the corresponding trajectories are denoted as $\mathbf{u}_i(\mathbf{f})$, $\mathbf{v}_i(\mathbf{f})$ and $\mathbf{x}_i(\mathbf{f})$. We also denote the performance of CAV i over the next H time steps under a given sequence $\mathbf{f}$ as $J_i^H(\mathbf{f})$. This OCP can then be efficiently tackled by solving a QP at each round. Next, we derive the CBF constraints for $\forall h \in \{1, \dots H\}$ which replace the original constraints.

Constraint 1 (Vehicle limitations): Let $b_1(\boldsymbol{x}_{i,h}) = v_{max} - v_{i,h}$, $b_2(\boldsymbol{x}_{i,h}) = v_{i,h} - v_{min}$. Following (8), the two corresponding CBF constraints are:

$$-u_{i,h} + \gamma_1(b_1(\boldsymbol{x}_{i,h})) \geq 0, \quad u_{i,h} + \gamma_2(b_2(\boldsymbol{x}_{i,h})) \geq 0 \quad (9)$$

Constraint 2 (Rear end safety constraint): Let $b_3(\boldsymbol{x}_{i,h}) = x_{i_p,h} - x_{i,h} - \varphi v_{i,h} - \delta$. Similarly, the CBF constraint is:

$$v_{i_p,h} - v_{i,h} - \varphi u_{i,h} + \gamma_3(b_3(\boldsymbol{x}_{i,h})) \geq 0 \quad (10)$$

Constraint 3 (Safe merging constraint): The safe merging constraint (4) only applies to specific time instants $t_{i_m}^k$. This poses a technical complication since that a CBF must be in a continuously differentiable form. We can convert (4) to a continuous time form using the technique in [3] to obtain:

$$z_{i,i_m}(t) \geq \frac{\varphi \cdot x_{i_m}(t)}{L} v_i(t) + \delta, \quad \forall t \in [t_i^{k,0}, t_{i_m}^k] \quad (11)$$

where $t_i^{k,0}$ denotes the time CAV i enters the road segment connected to M_k. Note that the boundary condition in (11) at $t = t_{i_m}^k$ when $x_{i_m}(t) = L$ is exactly (4). Letting $b_4(\boldsymbol{x}_{i,h}) = x_{i_m,h} - x_{i,h} - \frac{\varphi}{L}x_{i_m,h} \cdot v_{i,h} - \delta$, the CBF constraint is

$$v_{i_m,h} - v_{i,h} - \frac{\varphi}{L}x_{i_m,h} \cdot u_{i,h}$$
$$- \frac{\varphi}{L}v_{i_m,h} \cdot v_{i,h} + \gamma_4(b_4(\boldsymbol{x}_{i,h})) \geq 0 \quad (12)$$

Problem 2: Our aim is to calculate $J_i^H(\mathbf{f})$, $\mathbf{u}_i(\mathbf{f})$, $\mathbf{v}_i(\mathbf{f})$ and $\mathbf{x}_i(\mathbf{f})$ for a single CAV i given a sequence $\mathbf{f}$. Since the travel time $(t_i^f - t_i^0)$ in (7) can no longer be directly minimized in the receding horizon optimization process, we instead maximize the speed applying a linear (similar to $(t_i^f - t_i^0)$) penalty. Since this is inversely proportional to travel time when considering the entire CAV trip, we achieve an equivalent optimization effect:

$$\min_{\mathbf{u}_i} J_i^H(\mathbf{f}) = \sum_{h=1}^{H}(\frac{1}{2}u_{i,h}^2 - \lambda v_{i,h}) \quad (13)$$
$$s.t. \quad (1),(9),(10),(12)$$

where λ is a weight for balancing energy and speed.

3) MPC-CLBF framework: When the constraints (3)-(6) are initially satisfied, the forward invariance property of CBFs guarantees their satisfaction at all times. However, an unsafe initial state commonly occurs in a CZ when (4) is violated as the relative distance from the current position of CAV i to the next MP is similar to the distance from CAV i_m to the same MP. This motivates the use of *Control Lyapunov-Barrier Functions (CLBFs)* where a proper choice of class-$\mathcal{K}$ function allows us to achieve finite-time convergence to a safe set if a system is initially outside this set [16].

Although the continuous form (11) is used for the safe merging constraint, its satisfaction is only needed at the MP. Thus, if (11) is not satisfied before MP, there is some time over which the CAVs i and i_m can adjust their states and approach the safe set, instead of maximally decelerating to enforce feasibility as in earlier work [6], which implies expending energy and causes discomfort. In particular, the CLBF formulation for the safe merging constraint is:

$$L_f b_4(\boldsymbol{x}_i(t)) + L_g b_4(\boldsymbol{x}_i(t))u_i(t)$$
$$+ p \cdot b_4(\boldsymbol{x}_i(t))^q \geq 0, \quad \forall t \in [t_i^{k,0}, t_{i_m}^k] \quad (14)$$

where $b_4(\boldsymbol{x}_i(t)) = x_{i_m}(t) - x_i(t) - \frac{\varphi}{L}x_{i_m}(t) \cdot v_i(t) - \delta$ and the parameters p, q need to be properly selected.

p, q value determination. We define a safe merging set $C := \{\mathbf{x} \in \mathbb{R}^2 : b_4(\mathbf{x}) \geq 0\}$. If $\mathbf{x}_i(t) \in C$, we choose $p > 0$, $q = 1$, so that the last term of (14) reduces to a linear class-$\mathcal{K}$ function as in the formulation of a classic CBF constraint. Otherwise, if $\mathbf{x}_i(t) \notin C$, we set $p > 0$,

$q = \frac{1}{2n+1}$, $n \in \mathbb{Z}^+$. It is proved in [16] that any control satisfying (14) can force the state to converge to the safe set within time $t_m \geq t_{conv}$ where:

$$t_{conv} = \frac{b_4(\boldsymbol{x}_i(t))^{1-q}}{p(1-q)} \quad (15)$$

Setting $\bar{b}(t) = \frac{\varphi}{L}x_{i_m}(t)u_{i,min} + \frac{\varphi}{L}v_{i_m}(t)v_i(t) + v_i(t) - v_{i_m}(t)$, the following provides a sufficient condition for such finite time convergence, whose proof can be found in [13]:

Proposition 1: Given a safe set C and $\mathbf{x}_i(0) \notin C$, a feasible control $u_i(t) \geq u_{i,min}$ ensures $\mathbf{x}_i(t_m) \in C$ for any $t_m \geq t_{conv}$ if $u_i(t)$ satisfies (14) with $p \in [\frac{b_4(\boldsymbol{x}_i(0))^{1-q}}{(1-q)t_m}, \frac{\bar{b}(0)}{b_4(\boldsymbol{x}_i(0))^q}]$, and $q = \frac{1}{2n+1}$, $n \in \mathbb{Z}^+$.

In view of **Proposition** 1, we can choose proper p, q values in which we set the required convergence time t_m as the remaining time for CAV i_m to reach the next MP (this is known since we have already calculated the trajectory of CAV i_m). If we cannot find p, q values satisfying **Proposition** 1, then we cannot ensure that the associated control sequence is feasible and we proceed to consider the next sequence in the feasible sequence set $F_k(t)$.

After choosing proper p, q values, we can replace (12) by the CLBF constraint and replace **Problem 2** by **Problem 3**:

$$\min_{\boldsymbol{u_i}} J_i^H(\mathbf{f}) = \sum_{h=1}^H (\frac{1}{2}u_{i,h}^2 - \lambda v_{i,h})$$

$$s.t. \quad (1), (9), (10)$$

$$v_{i_m,h} - v_{i,h} - \frac{\varphi}{L}x_{i_m,h}u_{i,h} - \frac{\varphi}{L}v_{i_m,h}v_{i,h} + p \cdot (x_{i_m,h}$$
$$- x_{i,h} - \frac{\varphi}{L}x_{i_m,h}v_{i,h} - \delta)^q \geq 0, \quad \forall h \in \{1, \dots H\} \quad (16)$$

The solution is obtained in a decentralized way for each i in a given $\mathbf{f}$. This process is carried out sequentially, with the trajectories of preceding CAVs providing specific constraints for subsequent CAVs at each time step. We prioritize the CZ with the first CAV having the largest gap between conflicting vehicles, and then consider the upstream CZs.

Determine Optimal Sequence and Motion Control. Once we have evaluated the performance of each feasible sequence, the optimal sequence is chosen as the one with the best performance, i.e., $\mathbf{f}^* = \arg\min_{\mathbf{f}} \sum_{i \in \mathbf{f}} J_i^H(\mathbf{f})$. See [13] for the detailed procedure.

IV. SIMULATION RESULTS

In this section, we model a roundabout of the form in Fig. 1 in Eclipse SUMO, using its car-following model as a human-driven baseline to compare against our MPC-CLBF controller for CAVs. In addition, we compare with the OCBF controller from our previous work [14]. The OCBF controller first derives the unconstrained optimal solution as shown in Section III-.1. This solution is used as a reference control which is optimally tracked by minimizing quadratic control and speed deviations subject to the CBF constraints corresponding to (3)-(6). As in past work (e.g., [14]) this tracking is done by solving a sequence of QPs

at each discrete time step in a myopic way. This approach is computationally efficient but its myopic nature lacks the ability to predict future CAV behavior over multiple time steps as accomplished through the MPC-CLBF approach. Both First-In-First-Out (FIFO) and Shortest-Distance-First (SDF) sequencing policies are adopted under the OCBF controller, where SDF prioritizes a CAV with a smaller distance to the next MP and larger speed. We adopt the same configurations and vehicle arrival patterns in all methods for consistent comparison purposes. The basic parameter settings are as follows: $L = 60m$, $\delta = 0m$, $\varphi = 1.8s$, $v_{max} = 30m/s$, $v_{min} = 5m/s$, $u_{max} = 4m/s^2$, $u_{min} = -4m/s^2$.

Balanced traffic demand: In this case, the simulated incoming traffic is generated through Poisson processes with all rates set to 396 CAVs/h, with randomly assigned exit points. The simulation results are shown in Table II with all performance metrics for the total system and within each CZ using $\beta = 0.89$ in (7). The "infeasible count" denotes the number of times when no sequence is feasible for a merging group by solving **Problem 3**. This infeasibility is always due to conflicts between CLBF constraints and control limits when a new CAV enters the roundabout randomly, and no feasible p, q values can be found. The "unsafe count" denotes the number of times when the rear-end safety constraint (3) is violated by a CAV, which could happen due to insufficient space between a CAV and its conflicting CAV (i_m) at the next MP when CAV i_m just crossed the MP. Note that "unsafe" is only in terms of the conservative speed-dependent rear-end safety constraint rather than a physical collision. In fact, no collision is ever observed during our simulation experiments.

Table II shows that MPC-CLBF controllers outperform the SUMO (human-driven vehicle) baseline, as well as the OCBF controller under both sequencing policies in terms of travel time, energy consumption, and safety. The total objective value under MPC-CLBF with $H = 20$ shows 71.0%, 30.2% and 11.8% improvements compared to the SUMO baseline, OCBF with FIFO and SDF respectively, with the total energy consumption reduced by 94.1%, 72.4% and 24.5% respectively. The main reason that CAVs outperform Human-Driven Vehicles (HDVs) in terms of energy is that HDVs tend to drastically accelerate and decelerate in order to stop and wait for vehicles in another road segment to cross, or travel through the current road segment quickly when not seeing conflict vehicles. In addition, the MPC-CLBF method outperforms OCBF since it can predict future conflicts and preempt them with smoother control actions, avoiding maneuvers with drastic control changes.

An example of comparing trajectories for vehicle $i = 30$ is shown in Fig. 2. While the human-driven vehicles in the SUMO model tend to brake and accelerate sharply, the control for CAVs is much smoother. Compared to OCBF, speed varies less drastically with our method due to the ability of predicting future motion changes of other CAVs. In addition to saving energy, our method also allows faster roundabout traversal through reduced braking. In addition, we observe that the rear-end unsafe count is reduced by more than 99% compared to both SUMO and OCBF.
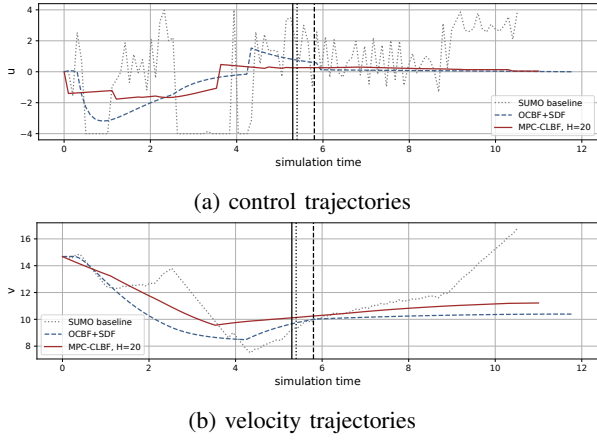
(a) control trajectories

(b) velocity trajectories

Fig. 2: Comparison of trajectories from vehicle 30

TABLE II: Performance Comparison under *Balanced* Traffic

Metric	total time	total energy	total obj.	infeasible count	unsafe count
SUMO Baseline	4425.7	12431.54	16365.50		7558
OCBF+FIFO	4657.6	2662.95	6803.04	404	1544
OCBF+SDF	4958.2	974.43	5381.72	343	449
MPC-CLBF, H=10	5033.3	898.54	5372.58	387	15
MPC-CLBF, H=20	4514.4	**735.81**	**4748.61**	**256**	4
MPC-CLBF, H=30	**4326.4**	989.59	4835.28	295	**3**

Unbalanced traffic demand: In this case, we set the traffic arrival rates to be 108 CAVs/h, 540 CAVs/h, and 540 CAVs/h for O_1, O_2 and O_3 respectively, so that the total traffic demand level for the whole roundabout is similar to the previous case. All other parameter settings are the same. Unlike the previous balanced case where MPC-CLBF with $H = 20$ was optimal, the total objective achieved now peaks at $H = 30$ using our MPC-CLBF method, demonstrating sensitivity to the traffic demand structure, which can be analyzed from historical statistics. Additional results under **unbalanced** and **heavy** traffic demand can be found in [13] suggesting that the MPC-CLBF controller is consistently robust to different traffic conditions.

Computational Complexity Analysis Let the number of CZs in a roundabout be N and the number of CAVs in the roundabout and entry road segments of CZ $k \in \{1, \ldots N\}$ be N_k^0 and N_k^1 respectively. It can be shown (see [13]) that the theoretical number of times to solve **Problem 3** can be expressed as $\sum_{k=1}^{N} \binom{N_k^0+N_k^1}{N_k^0} \cdot (N_k^0 + N_k^1)$, where N_k^0 and N_k^1 are bounded by the road segment length L. In our simulations, when $H = 30$, the average computation time for a single solution is around $100ms$ on an Intel Core m5 with two 1.2GHz cores using Gurobi as a numerical solver. This suggests the ability to adopt the MPC-CLBF controller for real time implementation.

V. CONCLUSION AND FUTURE WORK

We presented a decentralized MPC-CLBF framework which addresses both infeasibility and myopic control issues commonly encountered when coordinating CAVs over multiple interconnected CZs. This approach is then used to simultaneously determine the optimal sequence and associated control that jointly optimizes speed and energy consumption while guaranteeing safety. Future research is directed at sequencing and safe control over mixed-traffic scenarios where human-driven vehicles are involved.

REFERENCES

[1] Y. S. Chang, Y. J. Lee, and S. S. B. Choi, "Is there more traffic congestion in larger cities?-scaling analysis of the 101 largest us urban centers," *Transport Policy*, vol. 59, pp. 54–63, 2017.

[2] S. Liu, J. P. Petitti, Y. Lei, Y. Liu, and C. A. Shue, "By your command: Extracting the user actions that create network flows in android," in *14th International Conf. on Network of the Future*, 2023, pp. 118–122.

[3] W. Xiao and C. G. Cassandras, "Decentralized optimal merging control for connected and automated vehicles with safety constraint guarantees," *Automatica*, vol. 123, p. 109333, 2021.

[4] A. Li, A. S. C. Armijos, and C. G. Cassandras, "Cooperative lane changing in mixed traffic can be robust to human driver behavior," in *62nd IEEE Conf. on Decision and Control*, 2023, pp. 5123–5128.

[5] Y. Bichiou and H. A. Rakha, "Developing an optimal intersection control system for automated connected vehicles," *IEEE Trans. on Intelligent Transp. Systems*, vol. 20, no. 5, pp. 1908–1916, 2018.

[6] K. Xu and C. G. Cassandras, "Scaling up the optimal safe control of connected and automated vehicles to a traffic network: A hierarchical framework of modular control zones," in *26th IEEE Intelligent Transp. Systems Conf.*, 2023, pp. 1448–1453.

[7] L. A. Rodegerdts, *Roundabouts: An informational guide*. Transp. Research Board, 2010, vol. 672.

[8] Z. Farkas, A. Mihály, and P. Gáspár, "MPC control strategy for autonomous vehicles driving in roundabouts," in *Proc. of 30th Med. Conf. on Control and Automation*, 2022, pp. 939–944.

[9] M. Martin-Gasulla and L. Elefteriadou, "Single-lane roundabout manager under fully automated vehicle environment," *Transp. research record*, vol. 2673, no. 8, pp. 439–449, 2019.

[10] B. Chalaki, L. E. Beaver, and A. A. Malikopoulos, "Experimental validation of a Real-Time Optimal Controller for Coordination of CAVs in a Multi-Lane Roundabout," in *Proc. of IEEE Intelligent Vehicles Symposium*, 2020, pp. 775–780.

[11] L. García Cuenca, E. Puertas, J. Fernandez Andrés, and N. Aliane, "Autonomous Driving in Roundabout Maneuvers Using Reinforcement Learning with Q-Learning," *Electronics*, vol. 8, no. 12, p. 1536, 2019.

[12] A. P. Capasso, G. Bacchiani, and D. Molinari, "Intelligent Roundabout Insertion using Deep Reinforcement Learning," in *Proc. of 12th Intl. Conf. on Agents and Artificial Intelligence*, 2020, pp. 378–385.

[13] Y. Chen, C. G. Cassandras, and K. Xu, "Optimal sequencing and motion control in a roundabout with safety guarantees," *arXiv preprint arXiv:2403.09923*, 2024.

[14] K. Xu, C. G. Cassandras, and W. Xiao, "Decentralized time and energy-optimal control of connected and automated vehicles in a roundabout," in *Proc. of 24th IEEE Intelligent Transp. Systems Conf.*, 2021, pp. 681–686.

[15] M. H. B. M. Nor and T. Namerikawa, "Merging of connected and automated vehicles at roundabout using model predictive control," in *Proc. of 57th IEEE Annual Conf. of the Society of Instrument and Control Engineers of Japan*, 2018, pp. 272–277.

[16] W. Xiao, C. A. Belta, and C. G. Cassandras, "High order control lyapunov-barrier functions for temporal logic specifications," in *2021 IEEE American Control Conf.*, 2021, pp. 4886–4891.

[17] H. Xu, C. G. Cassandras, L. Li, and Y. Zhang, "Comparison of cooperative driving strategies for cavs at signal-free intersections," *IEEE Trans. on Intelligent Transp. Systems*, vol. 23, no. 7, pp. 7614–7627, 2021.

[18] K. Xu, C. G. Cassandras, and W. Xiao, "Decentralized time and energy-optimal control of connected and automated vehicles in a roundabout with safety and comfort guarantees," *IEEE Trans. on Intelligent Transp. Systems*, vol. 24, no. 1, pp. 657–672, 2022.

[19] A. Li, A. S. C. Armijos, and C. G. Cassandras, "Robust optimal lane-changing control for connected autonomous vehicles in mixed traffic," *arXiv preprint arXiv:2406.16870*, 2024.

[20] K. Vogel, "A comparison of headway and time to collision as safety indicators," *Accident analysis & prevention*, vol. 35, no. 3, pp. 427–433, 2003.

[21] W. Xiao, C. G. Cassandras, and C. Belta, *Safe Autonomy with Control Barrier Functions: Theory and Applications*. Springer Nature, 2023.